

Quasi-particle interaction in nuclear matter from chiral pion-nucleon dynamics

N. Kaiser

Physik-Department T39, Technische Universität München, D-85747 Garching, Germany

email: nkaiser@ph.tum.de

Abstract

Based on a recent chiral approach to nuclear matter we calculate the in-medium interaction of nucleons at the Fermi surface $|\vec{p}_{1,2}| = k_f$. The isotropic part of this quasi-particle interaction is characterized by four density-dependent (dimensionful) Fermi-liquid parameters: $f_0(k_f)$, $f'_0(k_f)$, $g_0(k_f)$ and $g'_0(k_f)$. In the approximation to 1π -exchange and iterated 1π -exchange (which as such leads already to a good nuclear matter equation of state) we find a spin-isospin interaction strength of $g'_0(2m_\pi) = 1.14 \text{ fm}^2$, compatible with existing empirical values. The consistency relations to the nuclear matter compressibility K and the spin/isospin asymmetry energies serve as a check on our perturbative calculation. In the next step we include systematically the contributions from 2π -exchange with virtual $\Delta(1232)$ -isobar excitation which have been found important for good single-particle properties and spin-stability of nuclear matter. Without any additional short-distance terms (contributing proportional to k_f^2) the spin-dependent Fermi-liquid parameters $g_0(k_{f0})$ and $g'_0(k_{f0})$ come out far too large. Estimates of these short-distance parameters from realistic NN-potentials go in the right direction, but sizeable enhancement factors are still needed to reproduce the empirical values of $g_0(k_{f0})$ and $g'_0(k_{f0})$. This points towards the importance of higher order iterations subsumed in the induced interaction. We consider also the tensor part of the quasi-nucleon interaction at the Fermi surface. In comparison to the leading 1π -exchange tensor interaction we find from the 2π -exchange corrections almost a doubling of the isoscalar tensor strength $h_0(k_f)$, whereas the isovector tensor strength $h'_0(k_f)$ is much less affected. These features are not changed by the inclusion of the chiral $\pi N\Delta$ -dynamics. The $l = 1$ tensor Fermi-liquid parameters $h_1(k_f)$ and $h'_1(k_f)$ follow a similar pattern.

PACS: 12.38.Bx, 21.30.Fe, 21.65.+f, 24.10.Cn

Keyword: Quasi-particle interaction in nuclear matter; Isotropic Fermi-liquid parameters; Tensor interaction; One- and two-pion exchange with medium modifications

1 Introduction and preparation

In recent years a novel approach to the nuclear matter problem based on effective field theory (in particular chiral perturbation theory) has emerged. Its key element is a separation of long- and short-distance dynamics and an ordering scheme in powers of small momenta. At nuclear matter saturation density $\rho_0 = 2k_{f0}^3/3\pi^2 \simeq 0.16 \text{ fm}^{-3}$ the Fermi momentum k_{f0} and the pion mass m_π are comparable scales ($k_{f0} \simeq 2m_\pi$), and therefore pions must be included as explicit degrees of freedom in the description of the nuclear many-body dynamics. The contributions to the energy per particle $\bar{E}(k_f)$ of isospin-symmetric (spin-saturated) nuclear matter as they originate from chiral pion-nucleon dynamics have been computed up to three-loop order in refs.[1, 2]. Both calculations are able to reproduce correctly the empirical saturation point of nuclear

matter by adjusting one single parameter (either a contact-coupling $g_0 + g_1 \simeq 3.23$ [1] or a cut-off $\Lambda \simeq 0.65$ GeV [2]) related to unresolved short-distance dynamics.¹ The novel mechanism for saturation in these approaches is a repulsive contribution to the energy per particle $\bar{E}(k_f)$ generated by Pauli blocking in second order (iterated) one-pion exchange. As outlined in section 2.5 of ref.[2] this mechanism becomes particularly transparent by taking the chiral limit $m_\pi = 0$. In that case the interaction contributions to $\bar{E}(k_f)$ are completely summarized by an attractive k_f^3 -term and a repulsive k_f^4 -term where the parameterfree prediction for the coefficient of the latter is very close to the one extracted from a realistic nuclear matter equation of state.

In a recent work [3] we have extended this chiral approach to nuclear matter by including systematically the effects from two-pion exchange with single and double virtual $\Delta(1232)$ -isobar excitation. The physical motivation for such an extension is threefold. First, the spin-isospin- $3/2$ $\Delta(1232)$ -resonance is the most prominent feature of low-energy πN -scattering. Secondly, it is well known that the two-pion exchange between nucleons with excitation of virtual Δ -isobars generates the needed isoscalar central NN-attraction [4] which in phenomenological one-boson exchange models is often simulated by a fictitious scalar "σ"-meson exchange. Thirdly, the delta-nucleon mass splitting $\Delta = 293$ MeV is of the same size as the Fermi momentum $k_{f0} \simeq 2m_\pi$ at nuclear matter saturation density and therefore pions and Δ -isobars should both be treated as explicit degrees of freedom. A large variety of nuclear matter properties has been investigated in this extended framework in ref.[3] and it has been found that the inclusion of the $\pi N\Delta$ -dynamics is able to remove most of the shortcomings of previous chiral calculations [2, 5] of nuclear matter. In particular, the momentum-dependence of the (real) single-particle potential $U(p, k_{f0})$ near the Fermi surface $p = k_{f0}$ improves significantly. The effective nucleon mass $M^* = 0.88M$ and thus the density of states at the Fermi surface are now better described. As a consequence the critical temperature of the liquid-gas phase transition is lowered to the realistic value $T_c = 15$ MeV. Moreover, the isospin properties improve also substantially by the inclusion of the chiral $\pi N\Delta$ -dynamics, as exemplified by the density dependence of the neutron matter equation of state $\bar{E}_n(k_n)$ and the asymmetry energy $A(k_f)$ (see Figs.10,11 in ref.[3]).

Given the fact that both groundstate and single-particle properties can be well described by perturbative chiral πN -dynamics up to three-loop order, it is natural to consider in a further step the in-medium interaction of quasi-nucleons (at the Fermi surface). Following this program we will therefore calculate in this work the density dependent Fermi-liquid parameters as they emerge from perturbative chiral pion-nucleon dynamics.

Fermi-liquid theory was invented by Landau [6] to describe strongly interacting (normal) many-fermion systems at low temperatures. At low excitation energies the elementary excitations of a many-fermion system are long-lived quasi-particles which in a certain sense interact weakly. The quasi-particles can thought of as free particles dressed by the interactions with the dense many-body medium. Landau's Fermi-liquid theory has been applied successfully to liquid ^3He [7], nuclear matter and nuclei [8]. In the latter case a set of Fermi-liquid parameters, describing the particle-hole interaction, is assigned to nuclei heavy enough to develop a central region of saturated nuclear matter. Via collective excitations of nuclei and magnetic multipole transitions, in particular the giant Gamow-Teller resonance, some of the nuclear Fermi-liquid parameters [9] can be determined from experimental data. Others are related to bulk properties of nuclear matter, such as its compression modulus $K = k_{f0}^2 \bar{E}''(k_{f0})$ or its (isospin) asymmetry energy $A(k_{f0})$. Various calculations of the nuclear Fermi-liquid parameters using Brueckner-Bethe theory and phenomenological nucleon-nucleon potentials have been performed in the

¹The cut-off scale Λ serves in ref.[2] the purpose to tune the strength of an emerging attractive zero-range NN-contact interaction.

past [9, 10, 11]. In ref.[12] the role of ρ -meson exchange for the spin-isospin parameter G'_0 has been emphasized. More recently, Schwenk et al. [13] have employed the renormalization group motivated universal low-momentum nucleon-nucleon potential $V_{\text{low-k}}$ [14]. In their work the induced interaction generated by the particle-hole parquet diagrams plays a very important role. In contrast to this rather sophisticated approach, ref.[15] takes into account only the bare potential $V_{\text{low-k}}$ or the in-medium G-matrix. The resulting Fermi-liquid parameters are then not in good agreement with empirical values (see Table 2 in ref.[15]). Moreover, saturation of nuclear matter could not be obtained with the potential $V_{\text{low-k}}$ in the Brueckner-Hartree-Fock approximation. According to recent work of Bogner et al. [16] the inclusion of the leading three-nucleon force from chiral effective field theory is essential in order to achieve reasonable saturation properties in this approach.

The purpose of the present paper is to explore the role of the long-range two-pion exchange for the nuclear Fermi-liquid parameters. We will restrict ourselves to the isotropic part of the quasi-nucleon interaction for which empirical information is best available [9, 13, 17]. To be specific, consider the angle-averaged quasi-particle interaction V_{eff} of two nucleons on the Fermi sphere, $|\vec{p}_1| = |\vec{p}_2| = k_f$. It is irreducible in the direct particle-hole channel and it has the following form:

$$\begin{aligned} \mathcal{F}_0(k_f) &= \frac{1}{(4\pi)^2} \int d\Omega_1 d\Omega_2 \langle \vec{p}_1, \vec{p}_2 | V_{\text{eff}} | \vec{p}_1, \vec{p}_2 \rangle \\ &= f_0(k_f) + g_0(k_f) \vec{\sigma}_1 \cdot \vec{\sigma}_2 + f'_0(k_f) \vec{\tau}_1 \cdot \vec{\tau}_2 + g'_0(k_f) \vec{\sigma}_1 \cdot \vec{\sigma}_2 \vec{\tau}_1 \cdot \vec{\tau}_2, \end{aligned} \quad (1)$$

where $|\vec{p}_1, \vec{p}_2\rangle$ stands for a properly anti-symmetrized two-nucleon state and $\vec{\sigma}_{1,2}$ and $\vec{\tau}_{1,2}$ denote the usual spin and isospin operators of the two nucleons. The density-dependent functions $f_0(k_f)$, $g_0(k_f)$, $f'_0(k_f)$ and $g'_0(k_f)$ of dimension fm^2 are the isotropic ($l=0$) Landau parameters. The spin- and isospin independent part $f_0(k_f)$ is alternatively given by the second functional derivative of the energy density with respect to the occupation density in momentum space [10]. Because of this property the Landau parameter $f_0(k_f)$ can be directly expressed in terms of the angle-integrated two-body and three-body kernels, $\mathcal{K}_2(p_1, p_2)$ and $\mathcal{K}_3(p_1, p_2, p_3)$, introduced in ref.[5] to facilitate the finite temperature calculation. For two-body and three-body contributions to $f_0(k_f)$ the following relations hold:

$$f_0(k_f)^{(2\text{-body})} = \frac{1}{8k_f^2} \mathcal{K}_2(k_f, k_f), \quad (2)$$

$$f_0(k_f)^{(3\text{-body})} = \frac{1}{(4\pi k_f)^2} \int_0^{k_f} dp p \left[\mathcal{K}_3(p, k_f, k_f) + \mathcal{K}_3(k_f, p, k_f) + \mathcal{K}_3(k_f, k_f, p) \right], \quad (3)$$

where the prefactors originate from the (convenient) normalization of the kernels $\mathcal{K}_{2,3}$ chosen in ref.[5]. For an interpretation of eqs.(2,3) note that in a diagrammatic language the second functional derivative is constructed by opening two nucleon lines of a closed in-medium diagram which represents the groundstate energy density. The relations eqs.(2,3) serve as a good check on our analytical one-loop calculation of the isotropic Landau parameters $f_0(k_f)$, $g_0(k_f)$, $f'_0(k_f)$ and $g'_0(k_f)$ to be presented in the next section.

2 Diagrammatic calculation of isotropic Fermi-liquid parameters

In this section we present analytical formulas for the density-dependent Fermi-liquid parameters $f_0(k_f)$, $g_0(k_f)$, $f'_0(k_f)$ and $g'_0(k_f)$ as derived from tree-level and one-loop pion-exchange

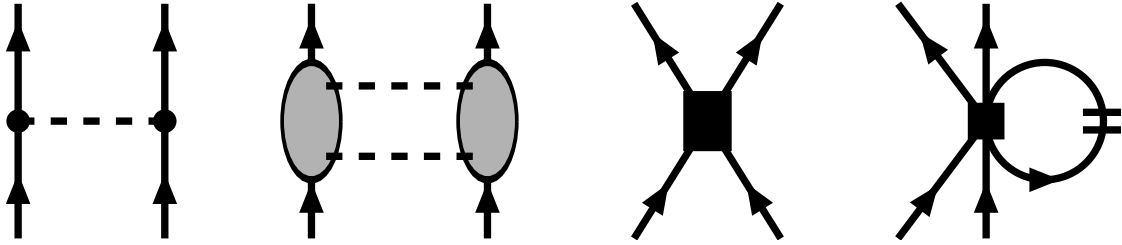


Figure 1: In-medium scattering diagrams related to one-pion exchange, irreducible two-pion exchange, a two-body contact interaction, and a three-body contact interaction.

diagrams. We give for each diagram only the final result omitting all technical details related to algebraic manipulations and solving elementary integrals. Diagrams can contribute via a direct term, where the ordering of \vec{p}_1 and \vec{p}_2 is the same in the initial and final state, and via a crossed term, where this ordering is reversed in the final state. In the latter case the negative product of the spin- and isospin exchange operators $-(1+S)(1+T)/4$ has to be multiplied from the left. Here, we have introduced the (convenient) short hand notations, $S = \vec{\sigma}_1 \cdot \vec{\sigma}_2$ and $T = \vec{\tau}_1 \cdot \vec{\tau}_2$, which we will use frequently in the following. The spin-spin and isospin-isospin operators satisfy the relations $S^2 = 3 - 2S$ and $T^2 = 3 - 2T$. We start now to enumerate the diagrammatic contributions to the angle-averaged quasi-particle interaction $\mathcal{F}_0(k_f)$ defined in eq.(1).

The crossed term from the (tree-level) one-pion exchange diagram in Fig.1 reads:

$$\mathcal{F}_0(k_f) = \frac{g_A^2}{48f_\pi^2}(3-S)(3-T) \left[1 - \frac{\ln(1+4u^2)}{4u^2} \right] \left(1 - \frac{k_f^2}{M^2} \right), \quad (4)$$

with the useful abbreviation $u = k_f/m_\pi$, where $m_\pi = 135$ MeV stands for the (neutral) pion mass. As usual $f_\pi = 92.4$ MeV denotes the weak pion decay constant and we choose the value $g_A = 1.3$ of the nucleon axial-vector coupling constant in order to have a pion-nucleon coupling constant of $g_{\pi N} = g_A M/f_\pi = 13.2$. Furthermore, $M = 939$ MeV denotes the (average) nucleon mass. The relativistic correction factor $1 - k_f^2/M^2$ in eq.(4) is not part of the diagram, but it stems from the squared M/E -prefactor in the relativistic density of states, with $E^2 = M^2 + k_f^2$. Consistency with the two-body kernel $\mathcal{K}_2^{(1\pi)}$ in eq.(5) of ref.[5] requires the inclusion this relativistic correction factor.

The left diagram in Fig.2 corresponds to iterated one-pion exchange. The direct term of this one-loop graph gives rise to the following (spin-independent) contribution:

$$\mathcal{F}_0(k_f) = \frac{g_A^4 M m_\pi}{512\pi f_\pi^4 u^2} (3-2T) \left[16u \arctan 2u - 5 \ln(1+4u^2) \right], \quad (5)$$

whereas its crossed term contributes in the form:

$$\begin{aligned} \mathcal{F}_0(k_f) = & \frac{g_A^4 M m_\pi}{3\pi(4f_\pi)^4 u^2} (3-5T) \left\{ \frac{1}{3}(3+S) \left[4u^2 - \ln(1+u^2) + (4u^3 + 6u) \arctan u \right] \right. \\ & \left. + (3-S) \left[\frac{1}{2} \ln(1+4u^2) - 2u \arctan 2u + \int_0^u dx \frac{\arctan 2x - \arctan x}{1+2x^2} \right] \right\}. \quad (6) \end{aligned}$$

Note the large scale enhancement factor M which stems from an energy denominator equal to the difference of small nucleon kinetic energies. The expressions in eqs.(5,6) do not include the

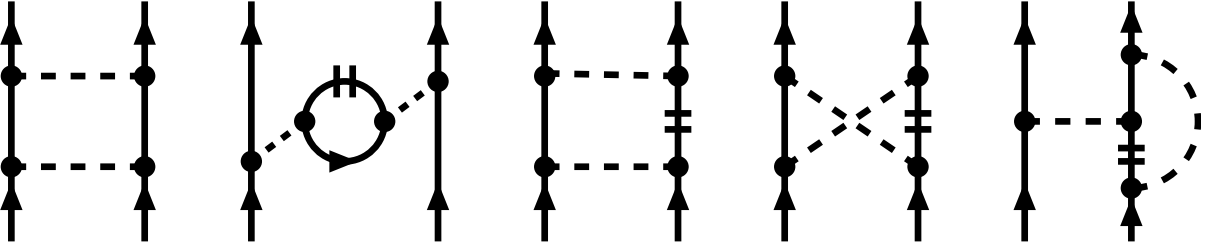


Figure 2: Iterated one-pion exchange and medium modifications of one-pion exchange and two-pion exchange. The short double-line symbolizes the filled Fermi sea of nucleons, i.e. the medium insertion $-\theta(k_f - |\vec{p}|)$ in the in-medium nucleon propagator [2]. Effectively, the medium insertion sums up hole-propagation and the absence of particle-propagation below the Fermi surface $|\vec{p}| < k_f$. Mirror graphs are not shown.

contribution of a linear divergence $\int_0^\infty dl 1$ of the momentum-space loop integral. If regularized by a cut-off scale Λ as done in ref.[2] one gets in addition the (constant) contribution:

$$\mathcal{F}_0(k_f) = \frac{g_A^4 M \Lambda}{128 \pi^2 f_\pi^4} (13T - 15 - 3S + 5ST), \quad (7)$$

which is equivalent to that of a (momentum-independent) NN-contact coupling. It turns out that with respect to the constraints from the empirical nuclear matter binding energy $\bar{E}(k_{f0})$ and asymmetry energy $A(k_{f0})$, one adjusted cut-off Λ is sufficient to represent the most general (i.e. two-parameter) contact-interaction at this order in the small momentum expansion. At higher orders there are of course more parameters to describe the short-distance dynamics (see eqs.(22,40) below).²

The remaining four graphs in Fig. 2 involve medium modifications as symbolized by the short double-line. The second diagram in Fig. 2 together with its mirror partner can be interpreted as a one-pion exchange modified by the coupling of the pion to nucleon-hole states. From its crossed term we derive the following contribution:

$$\mathcal{F}_0(k_f) = \frac{g_A^4 M m_\pi}{12 \pi^2 f_\pi^4 u^2} (3 - S)(3 - T) \int_0^u \frac{dx x^4}{(1 + 4x^2)^2} \left[2ux + (u^2 - x^2) \ln \frac{u+x}{u-x} \right]. \quad (8)$$

Pauli blocking acts in the planar and crossed 2π -exchange box diagrams in Fig. 2 (and their mirror partners). The direct term from the planar box diagram contributes in the form:

$$\mathcal{F}_0(k_f) = \frac{g_A^4 M m_\pi}{\pi^2 f_\pi^4 u^2} (3 - 2T) \int_0^u \frac{dx x^5}{(1 + 4x^2)^2} \left[u \ln \frac{u+x}{4(u-x)} + x \ln \frac{u^2 - x^2}{x^2} \right], \quad (9)$$

whereas the direct term from the crossed box diagram with Pauli blocking reads:

$$\mathcal{F}_0(k_f) = \frac{g_A^4 M m_\pi}{\pi^2 f_\pi^4 u^2} (3 + 2T) \int_0^u \frac{dx x^5}{(1 + 4x^2)^2} \left[u \ln \frac{4u^2}{u^2 - x^2} - x \ln \frac{u+x}{u-x} \right]. \quad (10)$$

Note that in both cases spin-dependent terms are absent. There is also the crossed term from the planar box with Pauli blocking. We split its contribution to $\mathcal{F}_0(k_f)$ into a factorizable part:

$$\mathcal{F}_0(k_f) = \frac{g_A^4 M m_\pi}{384 \pi^2 f_\pi^4} (3 + S)(3 - 5T) \int_0^u dx \left[1 + \frac{x^2 - u^2 - 1}{4ux} \ln \frac{1 + (u+x)^2}{1 + (u-x)^2} \right]^2, \quad (11)$$

²At N^3 LO, corresponding to two-loop order in NN-scattering, there are in total 24 short-distance coefficients [18].

and a non-factorizable part:

$$\begin{aligned} \mathcal{F}_0(k_f) = & \frac{g_A^4 M m_\pi}{48\pi^2 f_\pi^4 u^2} (3-S)(3-5T) \int_0^u \frac{dx x^3}{1+4x^2} \left[u \ln \frac{4(u-x)}{u+x} \right. \\ & \left. - x \ln \frac{u^2-x^2}{x^2} + \int_0^{u-x} \frac{dy}{\sqrt{R}} \ln \frac{u\sqrt{R} + (1-4xy)(x-y)}{u\sqrt{R} + (4xy-1)(x-y)} \right], \end{aligned} \quad (12)$$

with the auxiliary polynomial $R = 4u^2 + (4x^2 - 1)(4y^2 - 1)$. These two pieces are distinguished by whether the (remaining) nucleon propagator in the denominator can be canceled or not by terms from the product of πN -interaction vertices in the numerator. Finally, the last diagram in Fig. 2 (together with three mirror partners) represents a density-dependent vertex correction to the one-pion exchange. The non-vanishing contribution comes from the crossed term and we split again into a factorizable part:

$$\begin{aligned} \mathcal{F}_0(k_f) = & \frac{g_A^4 M m_\pi}{3\pi^2 (8f_\pi)^4 u^5} (3-S)(3-T) \left[4u^2 - \ln(1+4u^2) \right] \\ & \times \left[8u^4 + 4u^2 - (1+4u^2) \ln(1+4u^2) \right], \end{aligned} \quad (13)$$

and a non-factorizable part:

$$\begin{aligned} \mathcal{F}_0(k_f) = & \frac{g_A^4 M m_\pi}{3\pi^2 (4f_\pi)^4 u^2} (3-S)(3-T) \int_0^u dx \left[\ln(1+4x^2) - 4x^2 \right] \\ & \times \left\{ \ln \frac{u+x}{u-x} + \frac{1}{\sqrt{1+4u^2-4x^2}} \ln \frac{(u\sqrt{1+4u^2-4x^2}-x)^2}{(1+4u^2)(u^2-x^2)} \right\}. \end{aligned} \quad (14)$$

As can be seen from the power of m_π in their prefactors all contributions in eqs.(5,6,8-14) are of the same order in the small momentum expansion. The (bare) one-pion exchange eq.(4) and the contact term eq.(7) are (formally) of lowest order in the small momentum expansion.

The p-wave ($l=1$) Landau parameter $f_1(k_f)$, following $f_0(k_f)$ in the Legendre-polynomial expansion of the spin-isospin averaged quasi-nucleon interaction, is directly related to the slope of the (real) single-particle potential $U(p, k_f)$ at the Fermi surface [6, 10]:

$$f_1(k_f) = -\frac{3\pi^2}{2k_f^2} \left. \frac{\partial U(p, k_f)}{\partial p} \right|_{p=k_f}. \quad (15)$$

Its value at nuclear matter saturation density $\rho_0 = 2k_{f0}^3/3\pi^2$ determines the effective nucleon mass M^* via the relation:

$$M^* = M \left[1 - \frac{k_{f0}^2}{2M^2} - \frac{2Mk_{f0}}{3\pi^2} f_1(k_{f0}) \right]^{-1}. \quad (16)$$

The second term $-k_{f0}^2/2M^2$ in the square brackets stems from the relativistic correction $-p^4/8M^3$ to the kinetic energy. Although it is small, we keep this correction term for reasons of consistency with our earlier works [2, 3].

Fig. 3 shows the p-wave Landau parameter $f_1(k_f)$ as a function of the Fermi momentum k_f . The dashed curve corresponds to the approximation to 1π - and iterated 1π -exchange [2, 19]. The full curve includes in addition the higher order contributions from irreducible 2π -exchange with no, single and double virtual Δ -isobar excitation [3]. One should note that all short-distance parameters related to momentum-independent NN-contact interactions drop out in the

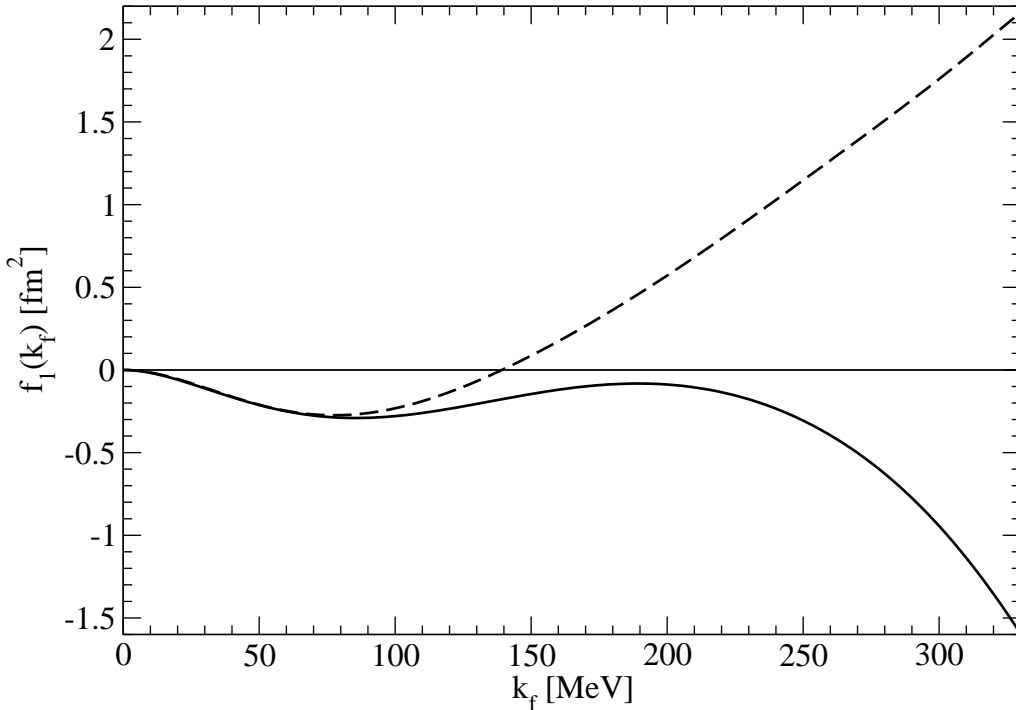


Figure 3: The p-wave Landau parameter $f_1(k_f)$ as a function of the Fermi momentum k_f . The dashed line corresponds to the approximation to 1π - and iterated 1π -exchange. The full line includes in addition the contributions from irreducible 2π -exchange with no, single and double virtual Δ -isobar excitation.

quantity $f_1(k_f)$. The remaining possible short-distance contribution $f_1(k_f)^{(ct)} = -5\pi^2 B_5 k_f^2 / M^4$ from the momentum-dependent NN-contact interactions (see eq.(9) in ref.[3]) plays numerically no role, since the adjustment to the saturation curve $\bar{E}(k_f)$ and the potential depth $U(0, k_{f0})$ gave as an optimal value $B_5 = 0$ [3]. The curves in Fig.3 display therefore the pure long-range effects from chiral one- and two-pion exchange. The upward bending of the dashed curve above $k_f \simeq 100$ MeV drives the p-wave Landau parameter $f_1(k_f)$ to a large positive value of $f_1(2m_\pi) \simeq 1.4 \text{ fm}^2$ at saturation density which translates into an unrealistically high effective nucleon mass of $M^* \simeq 2.9M$ at the Fermi surface. As one can see from the full line in Fig. 3 this wrong trend gets with increasing Fermi momentum k_f suppressed and finally reversed by the inclusion of the chiral $\pi N\Delta$ -dynamics. The negative value $f_1(k_{f0}) \simeq -0.4 \text{ fm}^2$ at saturation density $k_{f0} = 261.6 \text{ MeV}$ [3] is compatible with the empirical values of $f_1(k_{f0})$, collected in Table 1. As a consequence the effective nucleon mass at the Fermi surface takes on now a more realistic value: $M^* = 0.88M$. For Fermi momenta as large as $k_{f0} \simeq 2m_\pi$ the higher order corrections from the 2π -exchange with virtual Δ -excitation turn out to be essential for good single-particle properties. This feature which is exhibited here very clearly in Fig.3 is in agreement with the findings of ref.[3].

	f_0 [fm ²]	f_1 [fm ²]	f'_0 [fm ²]	g_0 [fm ²]	g'_0 [fm ²]
ref.[9]	-0.3...0	-0.75...0	0.9...1.5	small	1.6...1.7
ref.[17]	0.1	-0.6	0.7	1.12	1.41
ref.[13]	-0.29	-0.92	0.77	0.16 ± 0.3	1.1 ± 0.2

Tab.1: Empirical values of the (dimensionful) Landau parameters at nuclear matter saturation density $k_{f0} = 263 \text{ MeV}$ in units of fm². The dimensionless Landau parameters F_0, F_1 ,

F'_0 , G_0 , G'_0 have been divided by the density of states at the Fermi surface $N_0 = 2\pi^{-2}k_{f0}M^*$ taking for the effective nucleon mass $M^* = 0.8M$ [17] and $M^* = 0.72M$ [13], respectively. In the first row we used $N_0 = 1 \text{ fm}^{-2}$ (corresponding to $M^* = 0.78M$).

Next, we discuss the results for the isotropic Landau parameters $f_0(k_f)$, $g_0(k_f)$, $f'_0(k_f)$ and $g'_0(k_f)$ in the approximation to 1π - and iterated 1π -exchange. By adjusting the single cut-off scale Λ to the value $\Lambda = 611 \text{ MeV}$ this approximation leads already to a good nuclear matter equation of state with the saturation point at $\rho_0 = 0.173 \text{ fm}^{-3}$, $\bar{E}(k_{f0}) = -15.3 \text{ MeV}$, a nuclear matter compressibility of $K = k_{f0}^2 \bar{E}''(k_{f0}) = 252 \text{ MeV}$ [2, 19], and an (isospin) asymmetry energy of $A(2m_\pi) = 38.9 \text{ MeV}$. Fig. 4 shows the corresponding Landau parameters $f_0(k_f)$, $g_0(k_f)$, $f'_0(k_f)$ and $g'_0(k_f)$ (i.e. the summed contributions written in eqs.(4-14)) as a function of the Fermi momentum k_f . The strong density dependence of $f_0(k_f)$ including a sign change in the vicinity of saturation density k_{f0} is a generic feature which is also shared by many other calculations [9]. The other three Fermi-liquid parameters $g_0(k_f)$, $f'_0(k_f)$ and $g'_0(k_f)$ vary much less with the density $\rho = 2k_f^3/3\pi^2$ (or the Fermi momentum k_f). We read off from Fig. 4 at saturation density: $f_0(2m_\pi) = 0.55 \text{ fm}^2$, $g_0(2m_\pi) = -1.44 \text{ fm}^2$, $f'_0(2m_\pi) = 2.01 \text{ fm}^2$, and $g'_0(2m_\pi) = 1.14 \text{ fm}^2$. The negative value of $g_0(2m_\pi) = -1.44 \text{ fm}^2$ reflects the spin-instability of nuclear matter in this approximation, as discussed recently in ref.[20]. Although they lie outside their empirical ranges (see Table 1) the predicted values $f_0(k_{f0}) = 0.55 \text{ fm}^2$ and $f'_0(k_{f0}) = 2.01 \text{ fm}^2$ do obey the Landau relations [6, 10] to the nuclear matter compressibility:

$$K = 3k_{f0}^2 \left[\frac{1}{M^*} + \frac{2k_{f0}}{\pi^2} f_0(k_{f0}) \right], \quad (17)$$

and to the (isospin) asymmetry energy:

$$A(k_{f0}) = k_{f0}^2 \left[\frac{1}{6M^*} + \frac{k_{f0}}{3\pi^2} f'_0(k_{f0}) \right]. \quad (18)$$

The discrepancy comes of course from the much too high effective nucleon mass $M^* \simeq 2.9M$ in this approximation. The two spin-dependent Fermi-liquid parameters $g_0(k_{f0})$ and $g'_0(k_{f0})$ are connected by relations analogous to eq.(18) to the spin-asymmetry energy $S(k_{f0})$ and the spin-isospin asymmetry energy $J(k_{f0})$ [20]. We point out that in our calculation these (four) consistency relations hold with a numerical precision of one permille and better. It is also interesting to look at individual contributions. For example, the spin-isospin interaction strength $g'_0(2m_\pi)$ decomposes as $g'_0(2m_\pi) = (0.13 + 0.99 + 0.02) \text{ fm}^2 = 1.14 \text{ fm}^2$ into contributions from (static) 1π -exchange eq.(4), iterated 1π -exchange eqs.(6,7), and medium modified terms. Interestingly, the medium modified terms eqs.(8,11-14) sum up to a negligibly small net contribution. The important role of iterated 1π -exchange for the spin-isospin Fermi-liquid parameter $g'_0(k_f)$ has been stressed earlier in ref.[9]. The new element here is that this contribution is now evaluated consistently in a framework which leads to realistic nuclear matter binding and saturation. The predicted value $g'_0(2m_\pi) = 1.14 \text{ fm}^2$ of the spin-isospin Fermi-liquid parameter is compatible with existing empirical values (see Table 1). Nevertheless, it is clear from Fig. 3 that higher order corrections from 2π -exchange with virtual Δ -isobar excitation are essential in order to obtain good single-particle properties. Therefore we will now turn to the contributions of the chiral $\pi N \Delta$ -dynamics to the isotropic Fermi-liquid parameters $f_0(k_f)$, $g_0(k_f)$, $f'_0(k_f)$ and $g'_0(k_f)$.

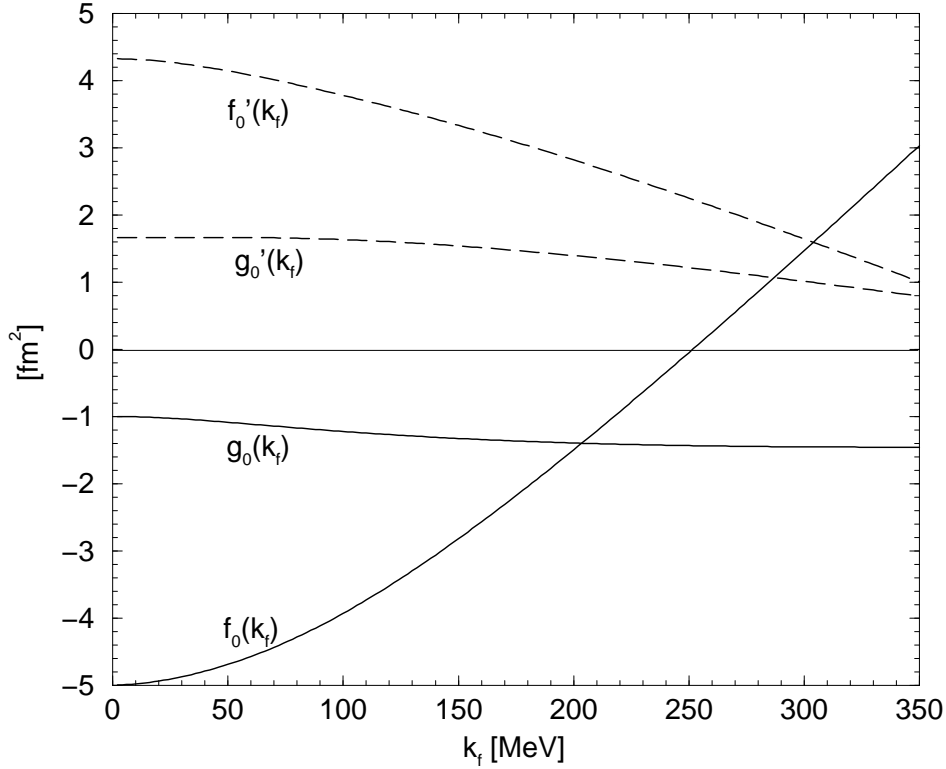


Figure 4: The isotropic Landau parameters $f_0(k_f)$, $g_0(k_f)$, $f'_0(k_f)$ and $g'_0(k_f)$ as a function of the Fermi momentum k_f . Only contributions from single and iterated pion exchange are included.

2.1 Two-pion exchange with virtual Δ -isobar excitation

The two-pion exchange nucleon-nucleon potential is symbolized by the second diagram in Fig. 1. We separate regularization dependent short-distance parts from the unique long-range terms with the help of a twice-subtracted dispersion relation. Applying this procedure to the crossed term of the (irreducible) 2π -exchange diagram in Fig. 1 we obtain a contribution to $\mathcal{F}_0(k_f)$ of the form:

$$\begin{aligned}
\mathcal{F}_0(k_f) = & \frac{1}{\pi} \int_{2m_\pi}^{\infty} d\mu \left[\frac{k_f^2}{\mu^3} - \frac{1}{2\mu} + \frac{\mu}{8k_f^2} \ln \left(1 + \frac{4k_f^2}{\mu^2} \right) \right] \left\{ \text{Im} \left(V_C + 3W_C + 2\mu^2 V_T + 6\mu^2 W_T \right) \right. \\
& + S \text{Im} \left(V_C + 3W_C - \frac{2}{3}\mu^2 V_T - 2\mu^2 W_T \right) + T \text{Im} \left(V_C - W_C + 2\mu^2 V_T - 2\mu^2 W_T \right) \\
& \left. + S T \text{Im} \left(V_C - W_C - \frac{2}{3}\mu^2 V_T + \frac{2}{3}\mu^2 W_T \right) \right\}, \quad (19)
\end{aligned}$$

where $\text{Im}V_C$, $\text{Im}W_C$, $\text{Im}V_T$ and $\text{Im}W_T$ are the spectral functions of the isoscalar and isovector central and tensor NN-amplitudes, respectively. Explicit expressions of these imaginary parts for the contributions of the triangle diagram with single Δ -excitation and the box diagrams with single and double Δ -excitation can be easily constructed from the analytical formulas given in section 3 of ref.[4]. The μ - and k_f -dependent weighting function in eq.(19) takes care that at low and moderate Fermi momenta this spectral integral is dominated by low invariant $\pi\pi$ -masses $2m_\pi < \mu < 1 \text{ GeV}$. The contributions to $\mathcal{F}_0(k_f)$ from irreducible 2π -exchange with only nucleon intermediate states can also be cast into the form eq.(19). The corresponding

non-vanishing spectral functions read [21]:

$$\text{Im}W_C(i\mu) = \frac{\sqrt{\mu^2 - 4m_\pi^2}}{3\pi\mu(4f_\pi)^4} \left[4m_\pi^2(1 + 4g_A^2 - 5g_A^4) + \mu^2(23g_A^4 - 10g_A^2 - 1) + \frac{48g_A^4 m_\pi^4}{\mu^2 - 4m_\pi^2} \right], \quad (20)$$

$$\text{Im}V_T(i\mu) = -\frac{6g_A^4\sqrt{\mu^2 - 4m_\pi^2}}{\pi\mu(4f_\pi)^4}. \quad (21)$$

The subtraction constants which come along with the twice-subtracted dispersion relation representation of the 2π -exchange nucleon-nucleon potential effectively parameterize a two-body contact interaction (see third diagram in Fig. 1). The direct and crossed term from the most general two-body contact interaction up to order- p^2 give rise together to the contribution:

$$\begin{aligned} \mathcal{F}_0(k_f) = & \frac{\pi^2}{M^2} \left\{ 3B_3 + S(B_3 - 6B_{n,3}) + T(6B_{n,3} - 3B_3) - ST B_3 \right\} \\ & + \frac{5\pi^2 k_f^2}{M^4} \left\{ B_5 + T(2B_{n,5} - B_5) + S B_5^\sigma + ST B_5^{\sigma\tau} \right\}. \end{aligned} \quad (22)$$

Note that the k_f -independent term in eq.(22) involves only two independent subtraction constants. This is a consequence of the Pauli exclusion principle (or the Fierz-antisymmetric nature of the two-body contact interaction). The four (dimensionless) parameters $B_3 = -7.99$, $B_{n,3} = -0.95$, $B_5 = 0$ and $B_{n,5} = -3.58$ have been adjusted in ref.[3] to empirical nuclear nuclear properties (such as the maximal binding energy per particle $-\bar{E}(k_{f0}) = 16$ MeV and the isospin asymmetry energy $A(k_{f0}) = 34$ MeV). We note as an aside that the constant contribution eq.(7) linear in the cut-off Λ is of course now not counted extra since the parameters B_3 and $B_{n,3}$ collect all such possible terms. The remaining two parameters B_5^σ and $B_5^{\sigma\tau}$ in eq.(22) are a priori not constrained by any groundstate properties of spin-saturated nuclear matter. We have also checked that the usual symmetries of the NN-interaction (isospin and Galilean invariance and Fierz-antisymmetry) do not imply a (linear) relation between the four parameters B_5 , $B_{n,5}$, B_5^σ and $B_5^{\sigma\tau}$.

In order to reduce a too strongly repulsive ρ^2 -term in the energy per particle $\bar{E}(k_f)$ a three-body contact interaction has been introduced in ref.[3]. The corresponding contribution to the quasi-particle interaction (represented by the last diagram in Fig. 1) is of the form:

$$\mathcal{F}_0(k_f) = \frac{g_A^4 \zeta k_f^3}{8\pi^2 \Delta f_\pi^4} (3 - S - T - ST), \quad (23)$$

with $\Delta = 293$ MeV the delta-nucleon mass splitting and the numerical parameter $\zeta = -3/4$. Here we have taken over from ref.[3] the parameterization of three-body contact-coupling strength. It is important to note here that the Pauli exclusion principle (together with isospin and rotational invariance) allows only for one single momentum-independent three-nucleon contact-coupling $\sim (\zeta g_A^4 / \Delta f_\pi^4) (\bar{N}N)^3$.

Fig. 5 shows additional pion-exchange diagrams with (single) virtual $\Delta(1232)$ -isobar excitation involving medium modifications. The first diagram in Fig. 5 can be interpreted as a one-pion exchange modified by the coupling to delta-hole states. Its crossed term gives rise to following the contribution:

$$\mathcal{F}_0(k_f) = \frac{g_A^4 m_\pi^3 u}{144\pi^2 \Delta f_\pi^4} (3 - S)(3 - T) \left[2u^2 + \frac{2u^2}{1 + 4u^2} - \ln(1 + 4u^2) \right], \quad (24)$$

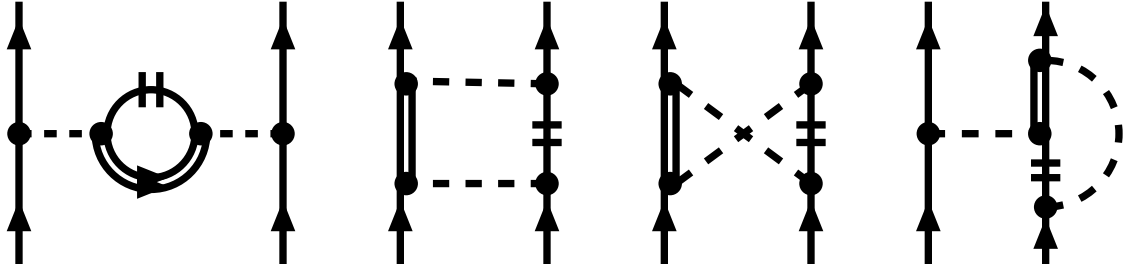


Figure 5: Medium modifications of one-pion exchange and two-pion exchange with excitation of virtual $\Delta(1232)$ -isobars. Mirror graphs are not shown.

with $u = k_f/m_\pi$, and we have already inserted the empirically well satisfied relation $g_{\pi N\Delta} = 3g_{\pi N}/\sqrt{2}$ for the $\pi N\Delta$ -coupling constant. The delta propagator shows up in this expression merely via the reciprocal mass splitting $\Delta = 293$ MeV. Pauli blocking acts in the second and third (planar and crossed) 2π -exchange box diagrams with Δ -excitation. The summed contribution of their direct terms is spin- and isospin independent:

$$\mathcal{F}_0(k_f) = \frac{g_A^4 m_\pi^3}{16\pi^2 \Delta f_\pi^4} \left[4u^3 - 12u + 15 \arctan 2u - \frac{9}{2u} \ln(1 + 4u^2) \right]. \quad (25)$$

On the other hand the summed contribution of their crossed terms can be written in the form:

$$\mathcal{F}_0(k_f) = -\frac{g_A^4 m_\pi^3}{64\pi^2 \Delta f_\pi^4} \int_0^u dx \left\{ 2X^2 + Y^2 + \frac{S+T}{3} (2X^2 + 7Y^2) + \frac{ST}{9} (10X^2 + 17Y^2) \right\}, \quad (26)$$

with the two auxiliary functions:

$$X = 2x - \frac{1}{2u} \ln \frac{1 + (u+x)^2}{1 + (u-x)^2}, \quad (27)$$

$$Y = \frac{5x^2 - 3u^2 - 3}{4x} + \frac{4x^2 + 3(1 + u^2 - x^2)^2}{16ux^2} \ln \frac{1 + (u+x)^2}{1 + (u-x)^2}. \quad (28)$$

Finally, the last diagram in Fig. 5 (together with three mirror partners) represents a density-dependent vertex correction to the one-pion exchange involving virtual Δ -excitation. The resulting contribution to $\mathcal{F}_0(k_f)$ from the crossed term reads:

$$\begin{aligned} \mathcal{F}_0(k_f) = & \frac{g_A^4 m_\pi^3}{9\pi^2 \Delta (4f_\pi)^4} (3-S)(3-T) \left\{ \frac{8}{u^2} \left[\ln(1 + 4u^2) - 4u^2 \right] \arctan 2u \right. \\ & + 35u - \frac{68u^3}{3} - \frac{3 + 4u^2}{4u^3} - \frac{3 + 16u^2 + 144u^4}{64u^7} \ln^2(1 + 4u^2) \\ & \left. + \frac{9 + 30u^2 - 12u^4 + 112u^6}{24u^5} \ln(1 + 4u^2) \right\}. \quad (29) \end{aligned}$$

Fig. 6 shows again the isotropic Fermi-liquid parameters $f_0(k_f)$, $g_0(k_f)$, $f'_0(k_f)$ and $g'_0(k_f)$ as a function of the Fermi momentum k_f , including now the new contributions written down in eqs.(19-29). One observes that the curve for $f_0(k_f)$ has approximately the same strong density dependence as before (compare with Fig. 4). The value $f_0(k_{f_0}) = 0.20$ fm² at saturation density ($k_{f_0} = 261.6$ MeV [3]) lies now much closer to its empirical range (see Table 1). The

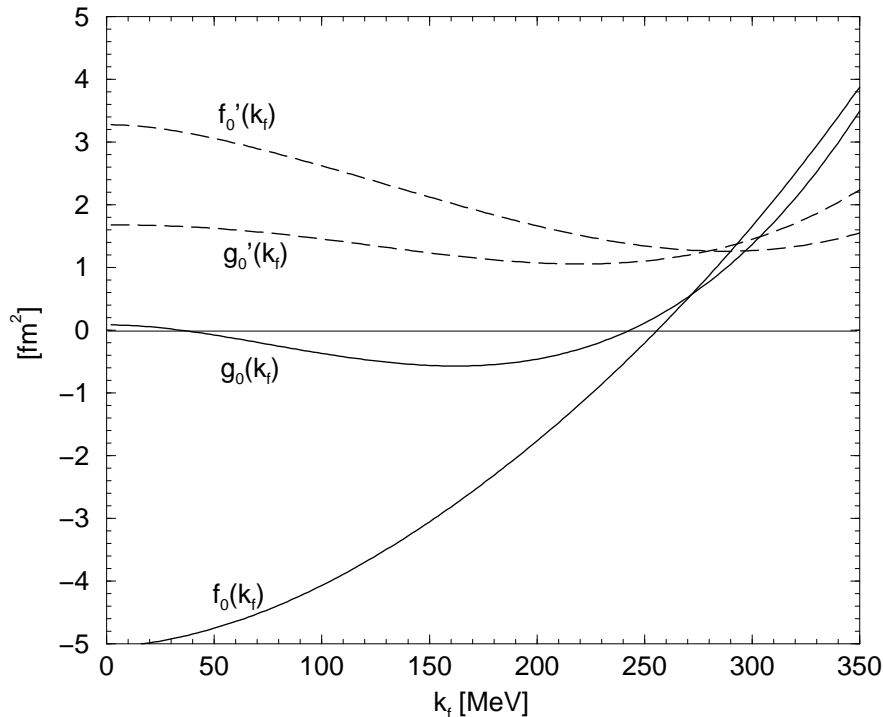


Figure 6: The isotropic Landau parameters $f_0(k_f)$, $g_0(k_f)$, $f'_0(k_f)$ and $g'_0(k_f)$ as a function of the Fermi momentum k_f . Contributions from two-pion exchange with excitation of virtual $\Delta(1232)$ -isobars are included in addition. The (spin-dependent) short-distance parameters have been set to the values $B_5^\sigma = -14$ and $B_5^{\sigma\tau} = -11$.

remaining overestimation of $f_0(k_{f0})$ is a consequence of the somewhat too high nuclear matter compressibility $K = 304$ MeV obtained in ref.[3]. The curves for $f_0(k_f)$ in Figs.4,6 are also quite instructive since they reveal that the smallness of the empirical $f_0(k_{f0})$ simply results from a zero-crossing of $f_0(k_f)$ in the near vicinity of nuclear matter saturation density. The isospin dependent Fermi-liquid parameter $f'_0(k_f)$ varies now less with density (compare Fig.6 with Fig.4) and it develops even a minimum at $k_f \simeq 290$ MeV. The resulting value at saturation density $f'_0(k_{f0}) = 1.30$ fm² lies within the empirically allowed range (see first row in Table 1). We note again that the consistency relations eqs.(17,18) hold with high numerical precision in our calculation. However, there are also the Pauli principle sum rules (see appendix A in ref.[9]). Due to their non-linear character these sum rules are most likely violated in the present perturbative approach.

Next, we discuss the spin-dependent Fermi-liquid parameters $g_0(k_f)$ and $g'_0(k_f)$. If one leaves out the k_f^2 -contributions proportional to the short-distance parameters B_5^σ and $B_5^{\sigma\tau}$ completely (i.e. setting $B_5^\sigma = B_5^{\sigma\tau} = 0$) one gets considerably too high values at saturation density, namely $g_0(k_{f0}) = 2.7$ fm² and $g'_0(k_{f0}) = 3.0$ fm². Relatively large contributions come from the twice-subtracted 2π -exchange potential eq.(19): $(2.33 S + 1.07 ST)$ fm², and the three-body term eq.(23): $(0.89 S + 0.89 ST)$ fm². The additional short-range dynamics encoded in the parameters B_5^σ and $B_5^{\sigma\tau}$ is therefore important in the spin-dependent channels. This is in line with ref.[12] where the role of ρ -meson exchange has been emphasized. In order to get an estimate of the short-distance parameters B_5^σ and $B_5^{\sigma\tau}$ we bring into play the complete set of four-nucleon contact-couplings written down in eqs.(3,4) of ref.[22]. This set represents the most general short-range NN-interaction quadratic in momenta and it involves seven low-energy constants C_1, \dots, C_7 . After computing the spin-dependent part of $\mathcal{F}_0(k_f)$ from the direct and

crossed term of the corresponding contact-potential we find:

$$\begin{aligned} B_5^\sigma &= \frac{M^4}{30\pi^2}(-3C_1 + 3C_3 + 3C_4 + C_6 + C_7) \\ &= \frac{M^4}{320\pi^3} \left[-6C(^1S_0) + 2C(^3S_1) - 3C(^1P_1) + C(^3P_0) + 3C(^3P_1) + 5C(^3P_2) \right], \quad (30) \end{aligned}$$

$$\begin{aligned} B_5^{\sigma\tau} &= \frac{M^4}{30\pi^2}(-3C_1 + 3C_3 + C_6) \\ &= \frac{M^4}{960\pi^3} \left[-6C(^1S_0) - 6C(^3S_1) + 9C(^1P_1) + C(^3P_0) + 3C(^3P_1) + 5C(^3P_2) \right]. \quad (31) \end{aligned}$$

In that form we obtain from the entries of Table IV in ref.[22] (corresponding to various realistic NN-potentials) the ranges $B_5^\sigma = -7.4 \dots -6.8$ and $B_5^{\sigma\tau} = -4.0 \dots -2.3$. It is gratifying that these estimates lead to sizeable negative values of the short-distance parameters B_5^σ and $B_5^{\sigma\tau}$, which are actually needed in order to reduce the far too high values of $g_0(k_{f0}) = 2.7 \text{ fm}^2$ and $g'_0(k_{f0}) = 3.0 \text{ fm}^2$ mentioned before. The curves in Fig.6 for the spin-dependent Fermi-liquid parameters $g_0(k_f)$ and $g'_0(k_f)$ have been calculated with $B_5^\sigma = -14$ and $B_5^{\sigma\tau} = -11$. This choice reproduces the empirical values $g_0(k_{f0}) = 0.34 \text{ fm}^2$ and $g'_0(k_{f0}) = 1.15 \text{ fm}^2$ of ref.[13]. Another welcome feature is that $g_0(k_f)$ does now not fall below -0.57 fm^2 and therefore the stability condition $2\pi^{-2}M^*k_f g_0(k_f) > -1$ [6, 10] is satisfied for all relevant densities. One can also see from Table 1 that the empirical value of $g_0(k_{f0})$ has a large uncertainty. In comparison to the lower ends of the foregoing estimate from realistic NN-potentials sizeable enhancement factors of about 1.9 and 2.8 need to be applied to the short-distance parameters B_5^σ and $B_5^{\sigma\tau}$. Obviously, our treatment of the short-range dynamics leaves here large errors. It should also be mentioned that most realistic NN-potentials (with the exception of $V_{\text{low-k}}$ [16]) require Brueckner resummation to yield meaningful results in nuclear matter.

The present calculation has still another shortcoming. According to earlier works [7, 10, 13, 23] the induced interaction (which sums planar exchange particle-hole diagrams to infinite order) is an important contribution to the quasi-particle interaction in nuclear matter. Some of the one-loop diagrams in Figs.2,5 do generate leading pion-exchange contributions to the induced interaction, but all the higher order iterations are consistently dropped here. In view of the good nuclear matter and single-particle properties obtained in the present perturbative framework one could argue that their effects in the spin-independent channels ($f_{0,1}(k_f)$ and $f'_0(k_f)$) are hidden in the adjusted values of the short-distance parameters. In the spin-dependent channels ($g_0(k_f)$ and $g'_0(k_f)$) the missing higher order iterations subsumed in the induced interaction may be the reason for the large mismatch remaining from the estimates of B_5^σ and $B_5^{\sigma\tau}$ from realistic NN-potentials. It should also be mentioned that the estimate $B_5 \simeq 7.8$ from these NN-potentials is not consistent with the optimal value $B_5 = 0$ of ref.[3].

3 Tensor interaction

In this section we investigate along the same lines as in section 2 the tensor part of the interaction of quasi-nucleons on the Fermi surface. The non-central (relative) tensor interaction has the following form [24]:

$$\frac{1}{4k_f^2} \left(3 \vec{\sigma}_1 \cdot \vec{q} \vec{\sigma}_2 \cdot \vec{q} - \vec{\sigma}_1 \cdot \vec{\sigma}_2 \vec{q}^2 \right) \sum_{l=0}^{\infty} \left[h_l(k_f) + h'_l(k_f) \vec{\tau}_1 \cdot \vec{\tau}_2 \right] P_l(\cos \vartheta), \quad (32)$$

with $\vec{q} = \vec{p}_1 - \vec{p}_2$ the difference between two (incoming or out-going) nucleon momentum vectors on the Fermi sphere $|\vec{p}_1| = |\vec{p}_2| = k_f$. The angular dependence of the tensor interaction strength is represented in eq.(32) by a series in Legendre-polynomials $P_l(\cos \vartheta)$ of $\cos \vartheta = \hat{p}_1 \cdot \hat{p}_2$. Again, we will restrict ourselves here to the (analytical) calculation to the leading ($l = 0$) Fermi-liquid parameters $h_0(k_f)$ and $h'_0(k_f)$ belonging to the tensor interaction. A first simplification arises from the observation that only crossed terms of pion-exchange diagrams can contribute to the tensor interaction. The different ordering of \vec{p}_1 and \vec{p}_2 in the initial and final state is a necessary condition for the spin-operators $\vec{\sigma}_{1,2}$ and the momentum transfer $\vec{q} = \vec{p}_1 - \vec{p}_2$ to survive in the diagrammatic amplitude. The contribution of the (bare) one-pion exchange is well known [9, 12]:

$$h_0(k_f) + T h'_0(k_f) = \frac{g_A^2}{24f_\pi^2} (3 - T) \ln(1 + 4u^2) \left(1 - \frac{k_f^2}{M^2} \right), \quad (33)$$

with $u = k_f/m_\pi$, and we have included the same relativistic correction factor as in eq.(4). The contribution from iterated one-pion exchange (see left diagram in Fig. 2) has the form:

$$h_0(k_f) + T h'_0(k_f) = \frac{g_A^4 M m_\pi}{3\pi(4f_\pi)^4} (3 - 5T) \left\{ 2 + \ln \frac{1 + u^2}{1 + 4u^2} - 2u \arctan u - \frac{1}{u} \arctan 2u + 2 \int_0^u dx \frac{\arctan 2x - \arctan x}{1 + 2x^2} \right\}, \quad (34)$$

and the next diagram where the pion couples to nucleon-hole states leads to the expression:

$$h_0(k_f) + T h'_0(k_f) = \frac{g_A^4 M m_\pi}{6\pi^2 f_\pi^4} (3 - T) \int_0^u \frac{dx x^2}{(1 + 4x^2)^2} \left[2ux + (u^2 - x^2) \ln \frac{u + x}{u - x} \right]. \quad (35)$$

More involved is the evaluation of the tensor component from the planar 2π -exchange box diagram with Pauli blocking (see third diagram in Fig. 2). We end up with the following triple integral representation:

$$h_0(k_f) + T h'_0(k_f) = \frac{g_A^4 M k_f}{96\pi^2 f_\pi^4} (3 - 5T) \int_0^1 dx \int_{-1}^1 dy \int_{-1}^1 dz \frac{x^2}{(u^{-2} + A)(u^{-2} + B)} \times \left\{ \frac{1}{2} + \frac{x^2 |y + z|}{A + B - 4} - \frac{(1 - x^2)^2 \text{sign}[(x - y)(x - z)] \theta(W)}{(A + B - 4) \sqrt{W}} \right\}, \quad (36)$$

with the auxiliary polynomials $A = 1 + x^2 - 2xy$, $B = 1 + x^2 - 2xz$ and $W = (x - y)^2(x - z)^2 - (1 - y^2)(1 - z^2)$. Finally, we have the last pion-exchange diagram in Fig. 2 with a density-dependent vertex correction. We split its contribution to the tensor Fermi liquid parameters into a factorizable part:

$$h_0(k_f) + T h'_0(k_f) = \frac{g_A^4 M m_\pi}{6\pi^2 (4f_\pi)^4 u^3} (3 - T) \ln(1 + 4u^2) \left[8u^4 + 4u^2 - (1 + 4u^2) \ln(1 + 4u^2) \right], \quad (37)$$

and a nonfactorizable part:

$$h_0(k_f) + T h'_0(k_f) = \frac{g_A^4 M m_\pi}{96\pi^2 f_\pi^4} (3 - T) \int_0^u dx \frac{\ln(1 + 4x^2) - 4x^2}{\sqrt{1 + 4u^2 - 4x^2}} \ln \frac{(u\sqrt{1 + 4u^2 - 4x^2} + x)^2}{(1 + 4u^2)(u^2 - x^2)}. \quad (38)$$

Fig. 7 shows the summed contributions eqs.(33-38) to the tensor Landau parameters $h_0(k_f)$ and $h'_0(k_f)$ as a function of the Fermi momentum k_f . We have dropped the small relativistic

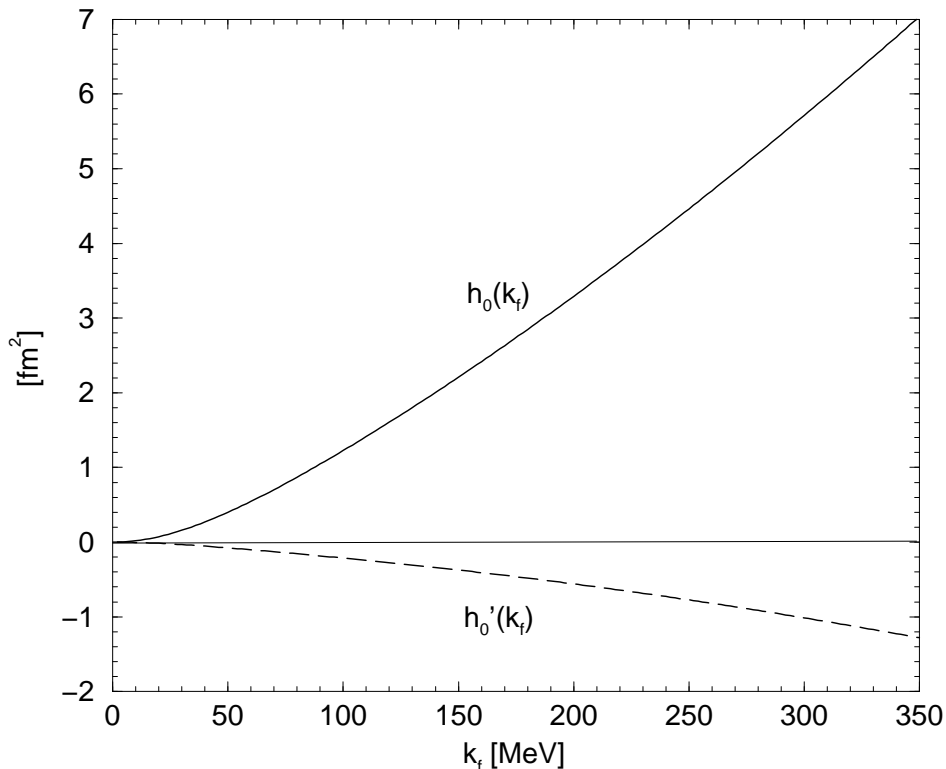


Figure 7: The Landau parameters $h_0(k_f)$ and $h'_0(k_f)$ related to the tensor interaction as a function of the Fermi momentum k_f . Only contributions from single and iterated pion exchange are included.

$1/M^2$ -correction to the 1π -exchange term eq.(33), since compared to the other contributions it is of higher order in the small momentum expansion. The solid and dashed line in Fig.7 correspond to the isoscalar $h_0(k_f)$ and isovector $h'_0(k_f)$ tensor interaction strength, respectively. Both curves start quadratically in k_f and above $k_f \simeq 100$ MeV a more linear behavior takes over. At nuclear matter saturation density $k_{f0} = 263$ MeV we obtain the values $h_0(k_{f0}) = 4.78 \text{ fm}^2$ and $h'_0(k_{f0}) = -0.83 \text{ fm}^2$. These numbers are to be compared with the leading tensor interaction from (static) 1π -exchange which gives $h_0(k_{f0})^{1\pi} = 2.68 \text{ fm}^2$ and $h'_0(k_{f0})^{1\pi} = -0.89 \text{ fm}^2$. Quite surprisingly, the (parameterfree) 2π -exchange corrections lead to almost a doubling of the isoscalar tensor strength $h_0(k_{f0})$, whereas the isovector tensor strength $h'_0(k_{f0})$ is much less affected. It is also instructive to see the individual contributions from the iterated 1π -exchange: $(-0.90 + 1.50 T) \text{ fm}^2$, the pion coupling to nucleon-hole states: $(3.75 - 1.25 T) \text{ fm}^2$, the planar box with Pauli blocking: $(0.33 - 0.55 T) \text{ fm}^2$, and the vertex correction: $(-1.08 + 0.36 T) \text{ fm}^2$. In comparison to these results previous works [12, 24] have found much smaller corrections to the one-pion exchange tensor interaction. The difference comes of course from our explicit treatment of the iterated pion-exchange (proportional to the large nucleon mass M) which is known to generate a sizeable tensor interaction (see eq.(32) in ref.[21]).

Next, we are interested in the effects of the chiral $\pi N\Delta$ -dynamics on the tensor interaction at the Fermi surface. The long-range part of the corresponding 2π -exchange NN-potential (symbolized by the second diagram in Fig.1) leads to the following contribution:

$$h_0(k_f) + T h'_0(k_f) = \frac{1}{3\pi} \int_{2m_\pi}^{\infty} d\mu \left[\mu \ln \left(1 + \frac{4k_f^2}{\mu^2} \right) - \frac{4k_f^2}{\mu} \right] \left\{ \text{Im}(V_T + 3W_T) + T \text{Im}(V_T - W_T) \right\}, \quad (39)$$

where $\text{Im}V_T$ and $\text{Im}W_T$ are the spectral functions of the isoscalar and isovector tensor NN-

amplitudes [4]. The short-range pieces are again encoded in two new subtraction constants:

$$h_0(k_f) + T h'_0(k_f) = \frac{k_f^2}{32\pi} \left\{ 2\sqrt{2}(1-T)C(\epsilon_1) + \frac{1}{3}(3+T) \left[3C(^3P_1) - 2C(^3P_0) - C(^3P_2) \right] \right\}. \quad (40)$$

From the entries in Table IV of ref.[22] we obtain the average values $C(\epsilon_1) = -3.95 \text{ fm}^4$ and $3C(^3P_1) - 2C(^3P_0) - C(^3P_2) = -20.5 \text{ fm}^4$, which will be used for the numerical evaluation of eq.(40). Additional contributions to the tensorial Landau parameters come from the diagrams in Fig. 5 involving Δ -excitations and medium modifications. The diagram where the pion couples to delta-hole states leads to the contribution:

$$h_0(k_f) + T h'_0(k_f) = \frac{g_A^4 k_f^3}{36\pi^2 \Delta f_\pi^4} (3-T) \left[\ln(1+4u^2) - \frac{4u^2}{1+4u^2} \right]. \quad (41)$$

Somewhat more involved is the evaluation of the (second and third) 2π -exchange box diagrams in Fig. 5 with Pauli blocking. We find the following representation:

$$\begin{aligned} h_0(k_f) + T h'_0(k_f) = & \frac{g_A^4 m_\pi^3}{96\pi^2 \Delta f_\pi^4} (3-T) \left\{ \frac{5u^3}{3} + \int_0^u dx \left[-\frac{2L}{u} \left((u^2 - x^2)^2 + u^2 + x^2 \right) \right. \right. \\ & + \frac{L^2}{u} \left(u(1+u^2-x^2)^2 + 4x^2(x-u)(1-ux+x^2) \right) \\ & \left. \left. + \int_{-1}^1 dy \frac{x^2(1+u^2+x^2)}{1+u^2+x^2-2uxy} \ln \frac{1+u^2+x^2+2uxy}{1+(u+x)^2} \right] \right\}, \quad (42) \end{aligned}$$

with the logarithmic auxiliary function:

$$L = \frac{1}{4x} \ln \frac{1+(u+x)^2}{1+(u-x)^2}. \quad (43)$$

The contribution of last pion-exchange diagram in Fig. 5 with a density dependent vertex correction can be given in closed analytical form:

$$\begin{aligned} h_0(k_f) + T h'_0(k_f) = & \frac{g_A^4 m_\pi^3}{9\pi^2 \Delta (4f_\pi)^4} (3-T) \left\{ -64 \ln(1+4u^2) \arctan 2u \right. \\ & - \frac{9+33u^2-192u^4+112u^6}{3u^3} \ln(1+4u^2) \\ & \left. + \frac{2}{u} (3+6u^2-8u^4) + \frac{3+16u^2+144u^4}{8u^5} \ln^2(1+4u^2) \right\}. \quad (44) \end{aligned}$$

Fig. 8 shows again the tensor Landau parameters $h_0(k_f)$ and $h'_0(k_f)$ as a function of the Fermi momentum k_f . We have now included the additional contributions eqs.(39-44) from the chiral $\pi N \Delta$ -dynamics and we have kept the relativistic k_f^2/M^2 -correction to the 1π -exchange term eq.(33). The solid and dashed lines in Fig. 8 for the isoscalar $h_0(k_f)$ and isovector $h'_0(k_f)$ tensor interaction strength are very similar to the previous ones in Fig. 7. At nuclear matter saturation density $k_{f0} = 263 \text{ MeV}$ we find now $h_0(k_{f0}) = 4.93 \text{ fm}^2$ and $h'_0(k_{f0}) = -0.69 \text{ fm}^2$. In comparison to the (static) 1π -exchange approximation this amounts again to almost a doubling of the tensor interaction strength in the isoscalar channel, whereas the isovector channel is much less affected. The short-distance term eq.(40) contributes to the total result at the level of about -11% . Its numerical value $(-0.56 + 0.08 T) \text{ fm}^2$ resembles the "weak" ρ -meson

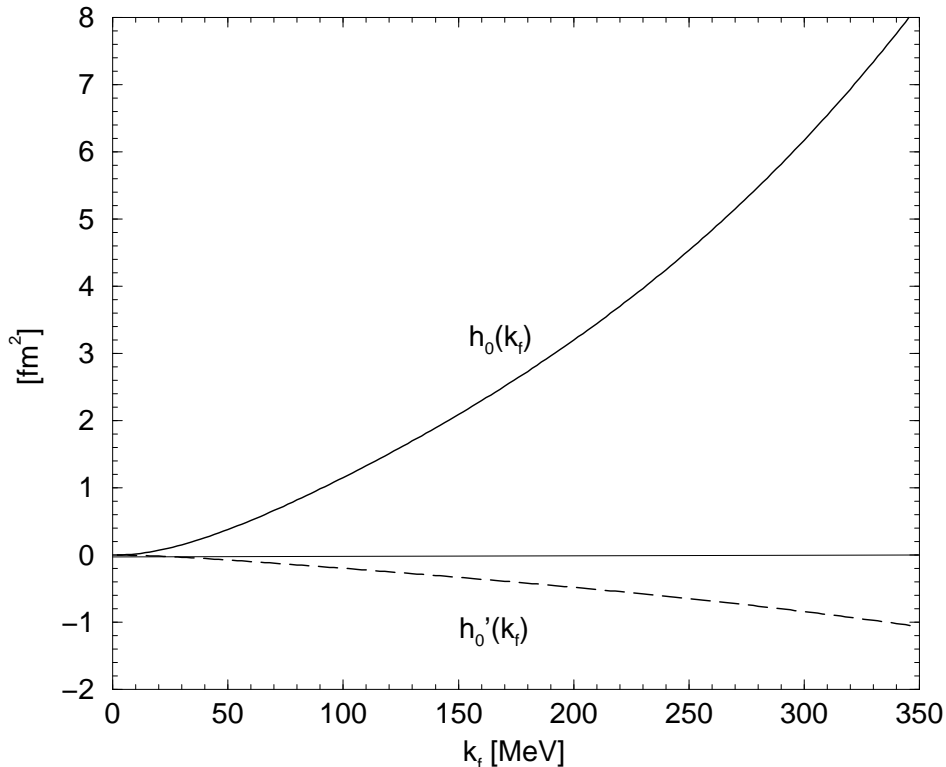


Figure 8: The Landau parameters $h_0(k_f)$ and $h'_0(k_f)$ related to the tensor interaction as a function of the Fermi momentum k_f . Contributions from two-pion exchange with excitation of virtual $\Delta(1232)$ -isobars are included in addition.

contribution of ref.[12] (see Table 1 therein). We conclude therefore that the sizeable effects of iterated 1π -exchange on the tensor interaction at the Fermi surface are not altered by higher order corrections from (irreducible) 2π -exchange with virtual Δ -isobar excitation and explicit short-distance contributions.

It is well known that the expansion in Legendre-polynomials eq.(32) converges slowly in case of the tensor interaction [12, 24]. For that reason we have calculated also the $l = 1$ tensor Fermi-liquid parameters $h_1(k_f)$ and $h'_1(k_f)$ in the present framework. The corresponding (numerical) results are shown as a function of the Fermi-momentum k_f in Fig. 9. The dashed lines correspond to the approximation to single and iterated pion-exchange and the full lines include in addition the (higher order) contributions from 2π -exchange with virtual $\Delta(1232)$ -isobar excitation. In comparison the leading contribution from (static) 1π -exchange:

$$h_1(k_f)^{1\pi} + T h'_1(k_f)^{1\pi} = \frac{g_A^2}{16f_\pi^2}(3 - T) \left[(2 + u^{-2}) \ln(1 + 4u^2) - 4 \right], \quad (45)$$

one finds a pattern similar to the $l = 0$ case. At nuclear matter saturation density $k_{f0} = 263$ MeV one has now from static 1π -exchange: $h_1(k_{f0})^{1\pi} + T h'_1(k_{f0})^{1\pi} = (3.33 - 1.11 T) \text{ fm}^2$. These numbers get enhanced to $h_1(k_{f0}) + T h'_1(k_{f0}) = (5.08 - 1.83 T) \text{ fm}^2$ by the iterated pion-exchange effects, whereas the further inclusion of contributions from 2π -exchange with virtual $\Delta(1232)$ -excitation leads only in minor changes: $h_1(k_{f0}) + T h'_1(k_{f0}) = (4.37 - 1.85 T) \text{ fm}^2$. One should also note that to the order in the small momentum expansion we are working here, $h_1(k_f)$ and $h'_1(k_f)$ receive no contribution from short-distance contact terms. We can therefore conclude that the features observed for the $l = 0$ tensor Fermi-liquid parameters are approximately repeated at $l = 1$ and presumably they continue to hold at higher l .

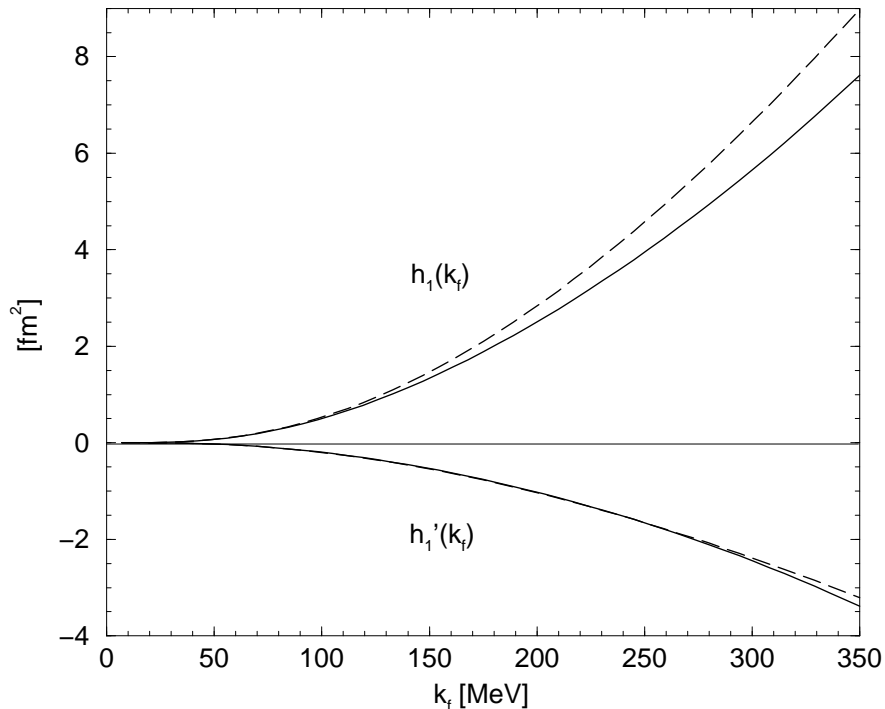


Figure 9: The Landau parameters $h_1(k_f)$ and $h'_1(k_f)$ related to the tensor interaction as a function of the Fermi momentum k_f . The dashed lines show contributions from single and iterated pion-exchange only. The full lines include also contributions from two-pion exchange with virtual $\Delta(1232)$ -isobar excitation.

4 Summary and conclusions

We have explored in this work the role of the long-range 2π -exchange for the in-medium interaction of quasi-nucleons at the Fermi surface $|\vec{p}_{1,2}| = k_f$. Our analytical calculation is rooted in a recent chiral approach to nuclear matter which can successfully explain binding and saturation of nuclear matter through two-pion exchange mechanisms [2, 3]. The isotropic part of the quasi-nucleon interaction is characterized by four density-dependent (dimensionful) Fermi-liquid parameters $f_0(k_f)$, $f'_0(k_f)$, $g_0(k_f)$ and $g'_0(k_f)$. In the approximation to 1π -exchange and iterated 1π -exchange we find a spin-isospin interaction strength of $g'_0(2m_\pi) = 1.14 \text{ fm}^2$, compatible with empirical values. The consistency relations to the nuclear matter compressibility K and the spin/isospin asymmetry energies are fulfilled in our perturbative calculation. However, the non-linear Pauli principle sum rules [9, 13] are most likely violated.

In the next step we have included in the quasi-particle interaction the contributions from 2π -exchange with virtual $\Delta(1232)$ -isobar excitation. This extension to higher orders in the small momentum expansion is necessary in order to obtain good single-particle properties and to guarantee spin-stability of nuclear matter [20]. Leaving out the short-distance terms (contributing proportional to k_f^2) the spin-dependent Landau parameters $g_0(k_{f0})$ and $g'_0(k_{f0})$ come out far too large. Estimates of these short-distance parameters from realistic NN-potentials go in the right direction, but sizeable enhancement factors are still needed to reproduce the empirical values of $g_0(k_{f0}) \simeq 0.34 \text{ fm}^2$ and $g'_0(k_{f0}) \simeq 1.15 \text{ fm}^2$ [13]. Another shortcoming of the present calculation is that only leading one-loop pion-exchange contributions to the induced interaction [7, 10, 12, 13, 23] could be included consistently. This is presumably the reason for our failure to describe the spin-dependent Fermi-liquid parameters, which are not constrained by any bulk properties of nuclear matter. Actually, one conclusion of ref.[25] has been that an

accurate description of the spin-response should include the induced interaction.

We have also considered the tensor part $3\vec{\sigma}_1 \cdot \vec{q} \vec{\sigma}_2 \cdot \vec{q} - \vec{\sigma}_1 \cdot \vec{\sigma}_2 \vec{q}^2$ of the quasi-nucleon interaction at the Fermi surface. In comparison to the leading 1π -exchange tensor interaction we have found from the iterated 1π -exchange corrections almost a doubling of the isoscalar tensor strength $h_0(k_f)$, whereas the isovector tensor strength $h'_0(k_f)$ was much less affected. This feature did not change qualitatively by the inclusion of the chiral $\pi N\Delta$ -dynamics. A similar pattern has been observed for the $l = 1$ tensorial Fermi-liquid parameters $h_1(k_f)$ and $h'_1(k_f)$.

4.1 Acknowledgements

I thank S. Fritsch for preparation of Fig. 3 and W. Weise for informative discussions.

References

- [1] M. Lutz, B. Friman and Ch. Appel, *Phys. Lett.* **B474** (2000) 7.
- [2] N. Kaiser, S. Fritsch and W. Weise, *Nucl. Phys.* **A697** (2002) 255; *Nucl. Phys.* **A700** (2002) 343.
- [3] S. Fritsch, N. Kaiser and W. Weise, *Nucl. Phys.* **A750** (2005) 259; nucl-th/0406038.
- [4] N. Kaiser, S. Gerstendörfer and W. Weise, *Nucl. Phys.* **A637** (1998) 395.
- [5] S. Fritsch, N. Kaiser and W. Weise, *Phys. Lett.* **B545** (2002) 73.
- [6] L.D. Landau, *Sov. Phys. JETP* **3** (1957) 920; **5** (1957) 101; **8** (1959) 70.
- [7] S. Babu and G.E. Brown, *Ann. Phys. (NY)* **78** (1973) 1.
- [8] A.B. Migdal, *Theory of Finite Fermi Systems and Applications to Atomic Nuclei*, Interscience, London, 1967.
- [9] S.O. Bäckman, G.E. Brown and J.A. Niskanen, *Phys. Rep.* **124** (1985) 1; and references therein.
- [10] O. Sjöberg, *Ann. Phys. (NY)* **78** (1973) 39.
- [11] W. Dickhoff, J. Meyer-ter-Vehn, H. Müther and A. Faessler, *Nucl. Phys.* **A368** (1981) 445; *Phys. Rev.* **C23** (1981) 1154.
- [12] G.E. Brown, S.O. Bäckman, E. Oset and W. Weise, *Nucl. Phys.* **A286** (1977) 191.
- [13] A. Schwenk, G.E. Brown and B. Friman, *Nucl. Phys.* **A703** (2002) 745.
- [14] S.K. Bogner, T.T.S. Kuo and A. Schwenk, *Phys. Rep.* **386** (2003) 1; and references therein.
- [15] J. Kuckei, F. Montani, H. Müther and A. Sedrakian, *Nucl. Phys.* **A723** (2003) 32.
- [16] S.K. Bogner, A. Schwenk, R.J. Furnstahl and A. Nogga, *Nucl. Phys.* **A763** (2005) 59.
- [17] S.O. Bäckman, A.D. Jackson and J. Speth, *Phys. Lett.* **B56** (1975) 209.
- [18] D.R. Entem and R. Machleidt, *Phys. Rev.* **C66** (2002) 014002; **C68** (2003) 041001.
- [19] S. Fritsch and N. Kaiser, *Eur. Phys. J.* **A17** (2003) 11.
- [20] N. Kaiser, *Phys. Rev.* **C70** (2004) 054001; **C72** (2005) 014007.
- [21] N. Kaiser, R. Brockmann and W. Weise, *Nucl. Phys.* **A625** (1997) 758.
- [22] E. Epelbaum, Ulf-G. Meißner, W. Glöckle, and C. Elster, *Phys. Rev.* **C65** (2002) 044001; and references therein.
- [23] J. Wambach, T.L. Ainsworth and D. Pines, *Nucl. Phys.* **A555** (1993) 128.
- [24] J. Dabrowski and P. Haensel, *Ann. Phys. (NY)* **97** (1976) 452.
- [25] A. Schwenk and B. Friman, *Phys. Rev. Lett.* **92** (2004) 082501.